August 27-31, 2023
FLORENCE - ITALY
ICWE 16
16th International Conference on Wind Engineering

Effect of the momentum provision on the low-occurrence wind velocity components at pedestrian levels around a simplified urban array

Toshiki Sanemitsu [1], Naoki Ikegaya [2]

[1]*Interdisciplinary Graduate school of Engineering Sciences, Kyushu University, Fukuoka, Japan, sanemitsu.toshiki@kyudai.jp*
[2]*Faculty of Engineering Sciences, Kyushu University, Fukuoka, Japan, ikegaya@cm.kyushu-u.ac.jp*

SUMMARY:
For solving wind environmental problems, the airflow over urban-like roughness has been studied using wind-tunnel experiments and computational fluid dynamics (CFD). In such CFDs, a part of developing boundary layers is extracted as a numerical domain using periodic boundary conditions in the horizontal direction to reproduce an infinite building array. The calculations need an artificial momentum source reproducing the developing boundary layer to drive the airflow such as a moving-lid and constant pressure gradient conditions. However, these methods do not appropriately reproduce the momentum supply mechanisms in developing boundary layers. Therefore, this study presents a new approach for driving the airflow, performs CFDs around a simplified roughness array using the four types of driving forces, and investigates the effect of the momentum provision on the wind environmental evaluation. Consequently, above the roughness sublayer (RSL), the momentum provisions cause the different vertical profiles of the Reynold stress and the skewness. In contrast, within the RSL, statistics become similar regardless of the methods. Accordingly, the peak factors of the streamwise and spanwise velocity components were determined to quantify the effect of the momentum provision on the rare but strong or weak wind speed distributions at a pedestrian level within an canopy.

Keywords: Urban boundary layer, Simplify block array, Momentum provision

1. INTRODUCTION

For solving the wind environmental problems, the relationship between the airflow at pedestrian levels and urban geometries has been studied for decades by means of both wind-tunnel experiment (WTE) and computational fluid dynamics (CFD) approaches. For such studies identifying genuine urban morphological effects on velocity fields, simplified urban-like arrays with sufficiently long fetch are commonly used to assume horizontal homogeneous boundary layers in WTEs. In CFDs, periodic boundary conditions in the horizontal direction are applied as the counterpart to reproduce infinitely repeated block arrays to form a horizontally homogeneous turbulent boundary layer. Although the simulation can reduce the numerical load thanks to the relatively smaller numerical domain than the size of an entire wind tunnel, it requires an artificial momentum source to drive airflow in the numerical domain. In previous studies, however, the airflows in such CFDs were driven as Couette or Hagen–Poiseuille flow, which differs from how the momentum is provided in turbulent boundary layers in WTEs. Consequently, it can be expected

that the momentum provision affects the turbulent statistics and probability density functions of the pedestrian-level wind velocity components. Therefore, we briefly explain the differences in the turbulent statistics by the airflows reproduced by large-eddy simulations (LESs) with four momentum provision methods. Accordingly, we investigate the influence of the momentum provisions on the occurrence of the rare velocity events showing their peak factors.

2. NUMERICAL DESCRIPTIONS

LESs were performed using OpenFOAM, which employs a finite volume method. The standard Smagorinsky model (the Smagorinsky constant $C_s = 0.12$) was used. The unsteady Semi-Implicit Method for Pressure Linked Equations, SIMPLE, algorithm was employed to couple the velocity components and pressure. The time step was 10^{-3}s. The temporal and spatial derivative terms were discretized by the second-order backward and linear interpolation schemes, respectively. Figure 1 (a) shows schematics of the calculation domain. The streamwise, spanwise, and vertical directions are defined as x, y, and z, and the corresponding wind speeds in each direction are defined as u, v, and w, respectively. The velocity components represent the resolved-scale quantities. The calculation domain was set to $4H \times 4H \times 4H$. Here, H represents the building height of $H = 0.1$m. Four cubes with the size of $H \times H \times H$ were arranged in a staggered array. The uniform grid resolution of $H/20$ was employed in each direction. Periodic boundary conditions were applied in both streamwise and spanwise directions, and no-slip boundary conditions were imposed on the floor of the domain and block walls. Four types of simulations with different momentum provisions were employed. Figure 1 (b) shows the vertical profiles of the momentum sources s_1 normalized by the total friction velocity u_τ defined by the total momentum source given to the domain. Case 1 imposes a constant streamwise wind speed on the upper surface as the boundary condition. Case 2 employs a constant streamwise pressure gradient via an external force. Case 3 and 4 are the conditions driven by the vertically varying momentum source in the momentum equation of the streamwise velocity component, which enables to reproduce the vertical momentum fluxes given in a referring CFD (Inagaki et al., 2017) or experiment (Harun et al., 2013) of developing boundary layers. The height-dependent momentum sources are expressed by empirically determined functions based on the Gaussian distribution and error function pair. In Case 2 to 4, free-slip boundary conditions were imposed on the upper surface of the domain. The sampling period was 275 s for Case 1 and 100 s for Case 2 to 4 after the initial calculation period of 200 s. The longer sampling period was required for Case 1 because the moving lid condition needs a longer period to remove the spatial non-uniformity. The velocity components were recorded at $40 \times 40 \times 40$ points in each direction with 1000 Hz.

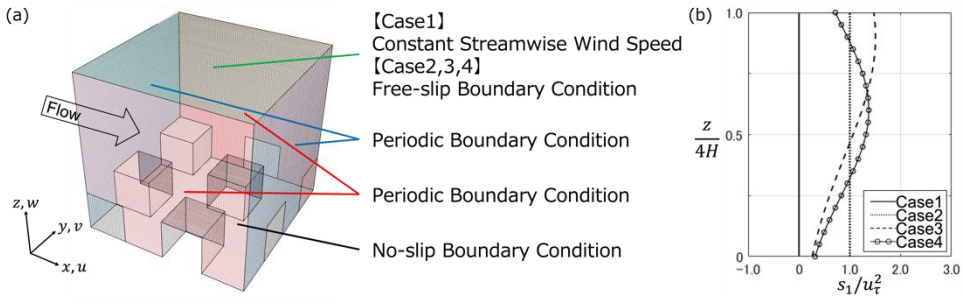

Figure 1. Numerical conditions. (a) Numerical domain and boundary conditions, and (b) the vertical profiles of momentum source s_1 in four cases. The values were normalized by the total friction velocity u_τ.

3. RESULTS

3.1. Statistics Distribution

Figure 2 (a) shows vertical profiles of the horizontally averaged Reynolds stress $-\langle\overline{u'w'}\rangle$. Here, $\overline{u_i}$ and $u_i' = u_i - \overline{u_i}$ are the temporal average and fluctuation part, and $\langle\overline{u_i}\rangle$ and $\overline{u_i}'' = \overline{u_i} - \langle\overline{u_i}\rangle$ is the horizontal average and deviation from the $\langle\overline{u_i}\rangle$. The Reynolds stress is normalized by the total friction velocity u_τ. In Fig. 2 (a), there are noticeable differences in the vertical profiles among four cases above $z/H > 1.2$, that is the expected to be the roughness sublayer (RSL) height, due to the momentum provision methods. This difference can be explained from the spatially and temporally averaged steady-state Navier–Stokes equation in the streamwise direction:

$$\partial_z\left(\langle\overline{u}''\overline{w}''\rangle + \langle\overline{u'w'}\rangle - \nu\partial_z\langle\overline{u}\rangle\right) = s_1(z) - f_1(z) \tag{1}$$

Here, f_1 represents the drag force acting on the canopy elements and bottom surfaces. The terms of $-\langle\overline{u}''\overline{w}''\rangle$ and $\nu\partial_z\langle\overline{u}\rangle$ are the dispersive and viscous stress, respectively. Equation (1) indicates that the total momentum flux in the vertical direction needs to balance with the momentum source s_1 (Fig. 1 (b)) and total drag force f_1. Since the viscous and dispersive stresses are smaller than Reynolds stress above the RSL, the Reynolds stress is directly determined by the momentum source s_1. Therefore, Fig. 2 (a) shows clear differnces of the Reynolds stress by reflecting the provided momentum source in each case. On the other hand, below the RSL, the difference among cases is small probably because the drag force has a greater influence on determining the Reynolds stress than the momentum source.

Figure 2 (b) shows the vertical profiles of the horizontally averaged skewness of three velocity components Sk_{u_i}. Above the RSL, although the skewness of the spanwise velocity component is nearly equal to zero due to the symmetric block array in the spanwise direction, the skewness of the streamwise and vertical velocity components slightly differs among cases. In Case 1, those have an approximately constant value of 0, whereas in Case 2 to 4, the skewness of streamwise and vertical velocity components becomes negative and positive, respectively, and tends to decrease and increase of the height. These results show that the momentum provision methods affect the stochastic properties of the airflow.

3.2. Pedestrian-Level Wind

Figure 3 compares the peak factors of the streamwise and spanwise velocity components u_{i_N}'/σ_{u_i}

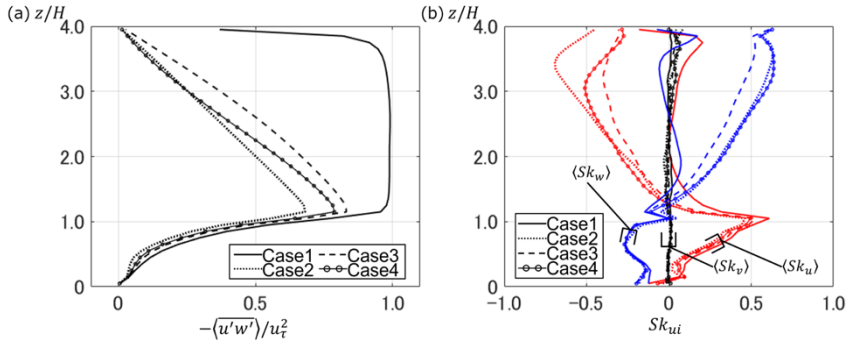

Figure. 2 Vertical profiles of horizontally averaged (a) Reynolds stress normalized by the total friction velocity u_τ and (b) skewness of three velocity components.

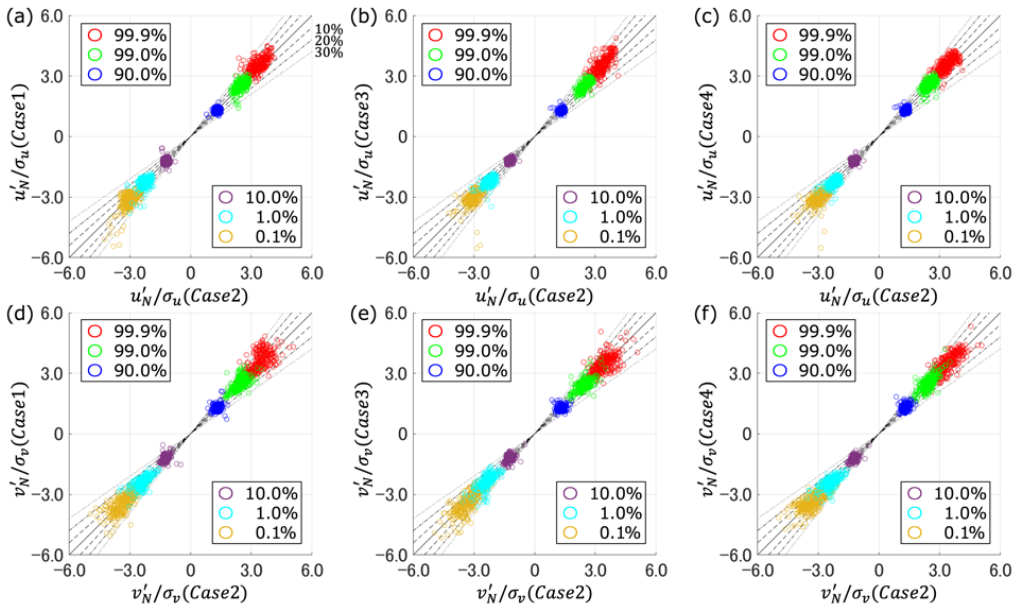

Figure 3. Correlation of peak factor of (a, b, c) streamwise and (d, e, f) spanwise velocity components at $z/H = 0.2$. (a, d), (b, e), and (c, f) are the comparisons between Case 2 and Case1, 3, and 4, respectively.

between Case 2 and other cases at $z/H = 0.2$. Here, ${u_i}'_N$ and σ_{u_i} represent the N percentile velocity and the standard deviation of velocity component. In Fig. 2 (b), the skewness of u and v agrees with each other regardless of the cases below the RSL. However, the peak factors in Case 1, 3, and 4 don't completely agree with those in Case 2. The expected maximum deviations among cases are almost 30%. In addition, rare but strong or weak winds represented by $N = 99.9$ and $N = 0.1$ show larger gap in all cases. Therefore, the fluctuations are affected by the momentum provision although the horizontally averaged airflow properties are consistent among cases.

4. CONCLUSION

We investigate the effect of the momentum provision on the turbulent statistics and percentile values at a pedestrian level. Above the RSL, the momentum provision affects the vertical profile of the Reynolds stress and skewness of velocity components. In contrast, within RSL, these statistics are not changed by the momentum provision. However, the horizontal distributions of the peak factor are different between driving forces. Therefore, in the RSL, the horizontally averaged airflow properties are unaffected by driving force, while their fluctuate parts are affected.

ACKNOWLEDGEMENTS

This work was partially supported by Grand-in-Aid for Scientific Research from JSPS, Japan, KAKENHI (Grant No. JP 17KK0117, JP 21K18770), FOREST program from JST (Grant No. JPMJFR205O), and JST SPRING (Grant No. JPMJSP2136).

REFERENCES

Harun, Z., Monty, J.P., Mathis, R., and Marusic, I., 2013. Pressure gradient effects on the large-scale structure of turbulent boundary layers. Journal of Fluid Mechanics 715, 477–498.

Inagaki, A., Kanda, M., et al, 2017. A numerical study of turbulence statistics and the structure of a spatially-developing boundary layer over a realistic urban geometry. Boundary-Layer Meteorology 164, 161–181.